

Research Article

In Vivo and in Vitro Analysis of Skin Penetration Enhancement Based on a Two-Layer Diffusion Model with Polar and Nonpolar Routes in the Stratum Corneum

Fumiyoshi Yamashita,¹ Hiroto Bando,¹ Yasuo Koyama,¹ Shuji Kitagawa,^{1,2} Yoshinobu Takakura,¹ and Mitsuru Hashida^{1,3}

Received January 21, 1993; accepted September 9, 1993

In vitro and *in vivo* skin penetration of three drugs with different lipophilicities and the enhancing effects of 1-geranylazacycloheptan-2-one (GACH) were studied in rats. *In vivo* drug absorption profiles obtained by deconvolution of urinary excretion profiles were compared to the corresponding *in vitro* data obtained with a diffusion experiment. *In vivo* skin penetration of lipophilic butylparaben was considerably greater than that observed *in vitro*, while hydrophilic mannitol and acyclovir showed low penetration in both systems without GACH pretreatment. On the other hand, GACH enhanced mannitol and acyclovir penetration, especially in the *in vivo* system. Analysis of absorption profiles, using a two-layer skin model with polar and nonpolar routes in the stratum corneum, suggested that the diffusion length of a viable layer (viable epidermis and dermis) was shorter *in vivo* than *in vitro* and the effective area of the polar route in the stratum corneum was larger *in vitro* without GACH pretreatment. GACH increased the partitioning of acyclovir into the nonpolar route to the same extent in both systems. In addition, GACH increased the effective area of the polar route *in vivo*, probably because of enhanced water permeability; however, this effect was smaller *in vitro* since the stratum corneum was already hydrated even without GACH pretreatment.

KEY WORDS: *in vitro* skin penetration; *in vivo* skin penetration; penetration enhancement; 1-geranylazacycloheptan-2-one; diffusion model; urinary excretion; deconvolution.

INTRODUCTION

In order to realize optimal transdermal drug delivery, adequate methodology for predicting percutaneous absorption is needed. In general, percutaneous absorption is a passive diffusion process and various mathematical models based on Fick's diffusion theory have been proposed, i.e., the parallel pathway model (1,2), multilayer model (3,4), and simultaneous diffusion and bioconversion model (5,6). A kinetic model for percutaneous absorption combined with systemic drug disposition has also been developed (7).

In most cases, however, percutaneous drug absorption has been studied with an *in vitro* diffusion experiment, since this allows direct measurement of skin penetration under the controlled condition. A goal of *in vitro* studies is the prediction of *in vivo* absorption behavior, and some attempts to predict it from *in vitro* data were reported based on a diffusion model (8–10) or using a convolution method (11). However, physicochemical and biological conditions of excised skin differ from those *in vivo*. In addition, skin permeation of

drugs may be affected *in vivo* by the microcirculation. Previous comparative *in vitro/in vivo* studies (12–15) failed to provide exact quantitative correlations, but some positive correlations were observed (13). Any theoretical study on *in vitro/in vivo* differences would require a model representing all processes of percutaneous drug absorption.

We have proposed that a two-layer skin model with polar and nonpolar routes in the stratum corneum could comprehensively account for *in vitro* skin permeation of drugs with different lipophilicities and effects of enhancers on them (16–20). This model enables us to discuss percutaneous drug absorption with parameters representing diffusion process through each domain.

The aim of the present study was to quantitate *in vitro/in vivo* differences in skin penetration and its enhancement. First, the barrier properties of skin to drug permeation were compared in terms of diffusion and partition parameters based on a diffusion model using three drugs with different lipophilicities, i.e., mannitol, acyclovir, and butylparaben. Next, the effects of an enhancer, 1-geranylazacycloheptan-2-one (GACH), were compared *in vitro* and *in vivo*.

MATERIALS AND METHODS

Materials. GACH was synthesized by Kuraray Co., Japan. Acyclovir was kindly supplied by the Wellcome Foundation, U.K. Mannitol (Nacalai Tesque Inc., Japan) and bu-

¹ Faculty of Pharmaceutical Sciences, Kyoto University, Yoshidashi-Imoadachi-cho, Sakyo-ku, Kyoto 606-01, Japan.

² Niigata College of Pharmacy, Kamishinei-cho, Niigata 950-21, Japan.

³ To whom correspondence should be addressed.

tylparaben (Tokyo Chemical Ind., Japan) were obtained commercially. [³H]Acyclovir, [¹⁴C]mannitol, and [¹⁴C]butylparaben were obtained from Daiichi Pure Chemicals, Japan.

In Vitro Skin Penetration Experiment. Full-thickness abdominal skin excised from a Wistar strain rat weighing about 200 g was used. After removal of hair, with a hair clipper, and of adipose tissue, the skin was punched out into a 3-cm-diameter disk and mounted on a flow-through-type diffusion cell with the epidermal side facing the donor cell (exposed area, 3.14 cm²) as described previously (20). The apparatus was thermostated at 37°C in a water bath throughout the experiment.

The skin mounted on the diffusion cell was pretreated with 0.2 ml of an ethanolic solution dissolving 0, 6.4, or 51.0 μmol of GACH. Six hours later, ethanol remaining in the donor cell was evaporated with a hair dryer and a 1-ml aliquot of the drug solution prepared by dissolving acyclovir, mannitol, or butylparaben at 1 mM in water was applied. The dermal side of the skin was continuously washed with saline containing streptomycin sulfate (50 mg/L; Sigma Chemical Co., St. Louis, MO) and penicillin G potassium salt (30 mg/L; gift from Toyo Jozo, Japan) which flowed at a rate of 12 mL/hr. The receptor fluid was collected every 45 min for 12 hr. At 12 hr after the start of the diffusion experiment, the drug remaining in the donor cell was recovered with about 8 mL of water. The skin was removed from the diffusion cell and a 1-cm-diameter disk was punched out to determine the drug content.

In vitro penetration through tape-stripped skin was also evaluated. After removal of hair with a clipper, the abdominal skin was stripped 15 times with adhesive tape (Scotch tape, Sumitomo 3M Co., Japan), excised, and punched out to yield a disk. The skin sample was mounted on a diffusion cell and pretreated with saline for 6 hr. Saline was then removed by blotting with tissue paper, and the drug was applied in a saline solution to reduce osmotic convective flow. The rest of the experimental procedures was the same as for intact skin.

Radioactivity was measured using a liquid scintillation counter (LSC-5000, Beckman, Japan). The radioactivity in the skin was measured after solubilization with Soluene-350 (Packard Instrument, IL).

In Vivo Skin Absorption. Under anesthesia induced by intraperitoneal injection of 1 g/kg urethane, the abdominal hair of a male Wistar strain rat weighing about 200 g was removed with an electric hair clipper and a glass half-chamber (effective area, 3.14 cm²) was attached to the abdominal surface using cyanoacrylate adhesive (Aron Alpha A, Sankyo Co., Japan) (21). GACH was pretreated in the same way as for the *in vitro* experiment. After pretreatment for 6 hr, the urinary bladder was cannulated with vinyl tubing (i.d., 0.50 mm; o.d., 0.90 mm; Dural Plastics & Engineering, Australia) and a 1-mL aliquot of drug solution was placed in the glass chamber. Urine was collected every 15 min for 4 hr by injecting 0.2 mL of 0.9% NaCl solution through the tubing twice before each sampling time. At the end of the experiment, the drug remaining in the donor cell was recovered and the skin was excised. After the urine and skin samples were solubilized, the radioactivity was measured.

Intravenous Injection. To determine the disposition of

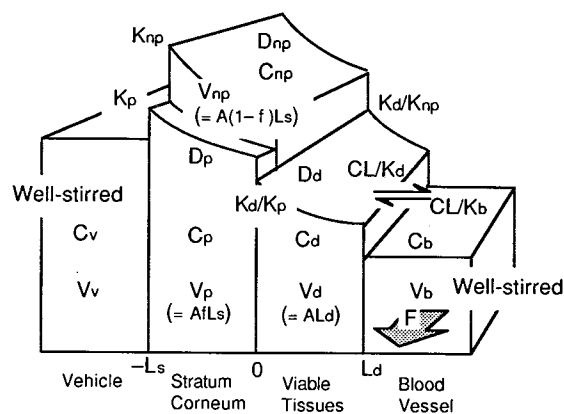


Fig. 1. A two-layer skin diffusion model with polar and nonpolar routes in the stratum corneum combined with the blood compartment. A well-stirred condition is assumed in the vehicle and blood compartment. *C*, drug concentration; *K*, partition coefficient; *D*, diffusion coefficient; *V*, volume; *L*, diffusion distance; *A*, effective area; *f*, area fraction of the polar route; *CL*, clearance through the capillary wall; and *F*, blood flow. Subscript v, vehicle; s, stratum corneum; p, polar route; np, nonpolar route; d, viable tissue; b, blood compartment. Note that each partition coefficient is defined against the vehicle.

the test drugs and estimate their absorption profiles through deconvolution (22), 0.2 mL of a 0.9% NaCl solution of each drug was injected into the femoral vein under urethane anesthesia. Urine was collected as described above to determine its radioactivity.

Data Analysis. Figure 1 shows a skin model composed of the first stratum corneum layer, with parallel polar and nonpolar routes, and the second viable layer. The viable layer and blood compartment are connected with "clearance." Vehicle and blood compartments are assumed to be under well-stirred conditions. In this model, drugs diffuse through the skin, reach the blood compartment, and transfer into the systemic circulation by blood flow.

The penetration profiles obtained in the *in vitro* study were analyzed based on a model in which a receptor phase under perfect sink conditions was connected with a viable layer (20). Based on this model, the Laplace transform for the amount of drug appearing in the receptor through the intact skin is expressed as follows (see the Appendix):

$$\tilde{Q} = Z_d X_0 (Z_{np} \sinh d_p + Z_p \sinh d_{np}) / s / g(s) \quad (1)$$

where *s* is the Laplace operator with respect to time; *X*₀ is the initially applied dose; and

$$d_p = L_s (s / D_p)^{1/2} \quad (2)$$

$$d_{np} = L_s (s / D_{np})^{1/2} \quad (3)$$

$$d_d = L_d (s / D_d)^{1/2} \quad (4)$$

$$Z_p = K_p V_p / d_p \quad (5)$$

$$Z_{np} = K_{np} V_{np} / d_{np} \quad (6)$$

$$Z_d = K_d V_d / d_d \quad (7)$$

$$g(s) = V_v (Z_p \cosh d_p \sinh d_{np} \sinh d_d + Z_{np} \sinh d_p \cosh d_{np} \sinh d_d + Z_d \sinh d_p \sinh d_{np} \cosh d_d) + Z_p \{ Z_p \sinh d_p \sinh d_{np} \sinh d_d$$

$$\begin{aligned}
& + Z_{np} \sinh d_d (\cosh d_p \cosh d_{np} - 1) \\
& + Z_d \cosh d_p \sinh d_{np} \cosh d_d \} + Z_{np} \\
& \{ Z_{np} \sinh d_p \sinh d_{np} \sinh d_d + Z_p \sinh d_d \\
& (\cosh d_p \cosh d_{np} - 1) + Z_d \sinh d_p \\
& \cosh d_{np} \cosh d_d \} \quad (8)
\end{aligned}$$

where V_v is the volume of vehicle; D_i , K_i , and V_i ($i = p, np, \text{ or } d$) are the diffusion coefficient in the i domain, the partition coefficient between the i domain and the vehicle, and the effective volume of the i domain for diffusion; and subscripts s, p, np, and d indicate the stratum corneum, polar route, nonpolar route, and second layer, respectively. V_i is obtained from the area (A), area fraction of the polar route (f), and diffusion length (L_i) as

$$V_p = AfL_s \quad (9)$$

$$V_{np} = A(1 - f)L_s \quad (10)$$

$$V_d = AL_d \quad (11)$$

In vivo absorption was also analyzed by the same model since the major barrier to diffusion is in the stratum corneum and the blood flow should have little effect on the penetration of drugs unless it is drastically reduced (23). This enables us to compare *in vivo* and *in vitro* systems with the same parameters. Curve-fitting to *in vivo* data was performed for a urinary excretion profile in order to minimize the error incurred during numerical calculation (21). Expressing the excretion profile by a biexponential function ($dX_u/dt = A * e^{-\alpha t} + B * e^{-\beta t}$), the Laplace transformed equation for urinary excretion of topically applied drug is as follows:

$$\bar{X}_u = \bar{Q} * \{A/(s + \alpha) + B/(s + \beta)\} \quad (12)$$

This equation was fitted to urinary excretion data after topical application. Curve-fitting to data was performed using the nonlinear regression program with a fast inverse Laplace transform algorithm MULTI(FILT) (24) on the M-382 mainframe computer at the Kyoto University Data Processing Center.

Because of the difficulty in determining the real diffusion length, we defined two parameters for drug diffusion and partitioning involving the diffusion length as follows (17,19,20):

$$D'_i = D_i/L_i^2 \quad (13)$$

$$K'_i = K_i V_i \quad (i = p, np, \text{ or } d) \quad (14)$$

The six targeted hybrid parameters for each drug were determined according to procedures reported previously (20). In this analysis, three assumptions were introduced: (i) The polar route is filled with water and the partition coefficient between the polar route and the aqueous vehicle is unity, (ii) diffusion in the polar route obeys the Einstein-Stokes equation, and (iii) GACH dose not affect the permeability of the viable layer.

RESULTS

In Vitro Absorption. Figure 2 shows the *in vitro* penetration profiles of mannitol, acyclovir, and butylparaben.

Penetration of mannitol, a very hydrophilic drug, was barely enhanced by pretreatment with GACH. For acyclovir with an octanol-water partition coefficient ($PC_{oct/w}$) of 0.0304, penetration was significantly increased only by pretreatment with 51.0 μmol of GACH. For butylparaben, a lipophilic drug, penetration decreased with increasing GACH dose. Table I summarizes the amount of each drug recovered in the donor phase, skin, and receptor phase at the end of a 12-hr diffusion experiment. The amount of drugs in the skin, normalized to the total recovery, increased monotonously with increasing GACH dose. The total recoveries of butylparaben were relatively low due to its adsorption onto the donor cell (19).

In Vivo Absorption. Urinary excretion profiles of drugs after intravenous injection were approximated with a biexponential function as follows by least-square regression analysis:

$$dX_u/dt = 146 * \exp(-2.24 * t) + 17.8 * \exp(-0.689 * t) \quad (\text{for mannitol})$$

$$dX_u/dt = 166 * \exp(-2.61 * t) + 17.4 * \exp(-0.666 * t) \quad (\text{for acyclovir})$$

$$dX_u/dt = 250 * \exp(-6.75 * t) + 69.7 * \exp(-1.05 * t) \quad (\text{for butylparaben})$$

where dX_u/dt expresses the urinary excretion rate (% of dose/hr).

In vivo absorption profiles obtained by a deconvolution method are also shown in Fig. 2. The lag-time phase was shorter *in vivo* than *in vitro* for each penetration profile. In addition, absorption of these drugs was higher *in vivo* than *in vitro* in most cases. Table II summarizes amount of drug recovered in the donor, skin, and urine and the calculated amount of systematically absorbed drugs at the end of 4-hr absorption experiment. In contrast to the *in vitro* results, *in vivo* penetration of mannitol and acyclovir was strongly enhanced by GACH. Although the penetration of butylparaben was also decreased by GACH in the *in vivo* experiment, the extent of the decrease was less than *in vitro*. GACH increased the amount of drug in skin in the *in vivo* system as well as *in vitro*, suggesting that the action mechanism of GACH was similar *in vitro* and *in vivo*.

Analysis of Penetration Profiles Based on a Two-Layer Skin Model with Polar and Nonpolar Routes in the Stratum Corneum. Table III summarizes *in vitro* and *in vivo* penetration parameters of mannitol and acyclovir for the polar route, nonpolar route, and lower viable layer. Since the total recovery of butylparaben in the *in vivo* experiment remained low (Table II), analysis was not done for this compound. Without GACH pretreatment, diffusion parameters in the viable layer were larger in the *in vivo* system than *in vitro* for all drugs, while partition parameters were smaller in the *in vivo* system.

Parameters for the polar route were estimated assuming that mannitol, a highly hydrophilic drug, diffuses only through the polar route in the stratum corneum (2,20,25,26). Without GACH pretreatment, the partition parameter in the polar route *in vitro* was 10-fold larger than *in vivo*, while diffusion parameters were similar. Pretreatment with 51.0 μmol GACH increased the partition parameters in the polar route 2- and 24-fold over the control *in vitro* and *in vivo*, respectively.

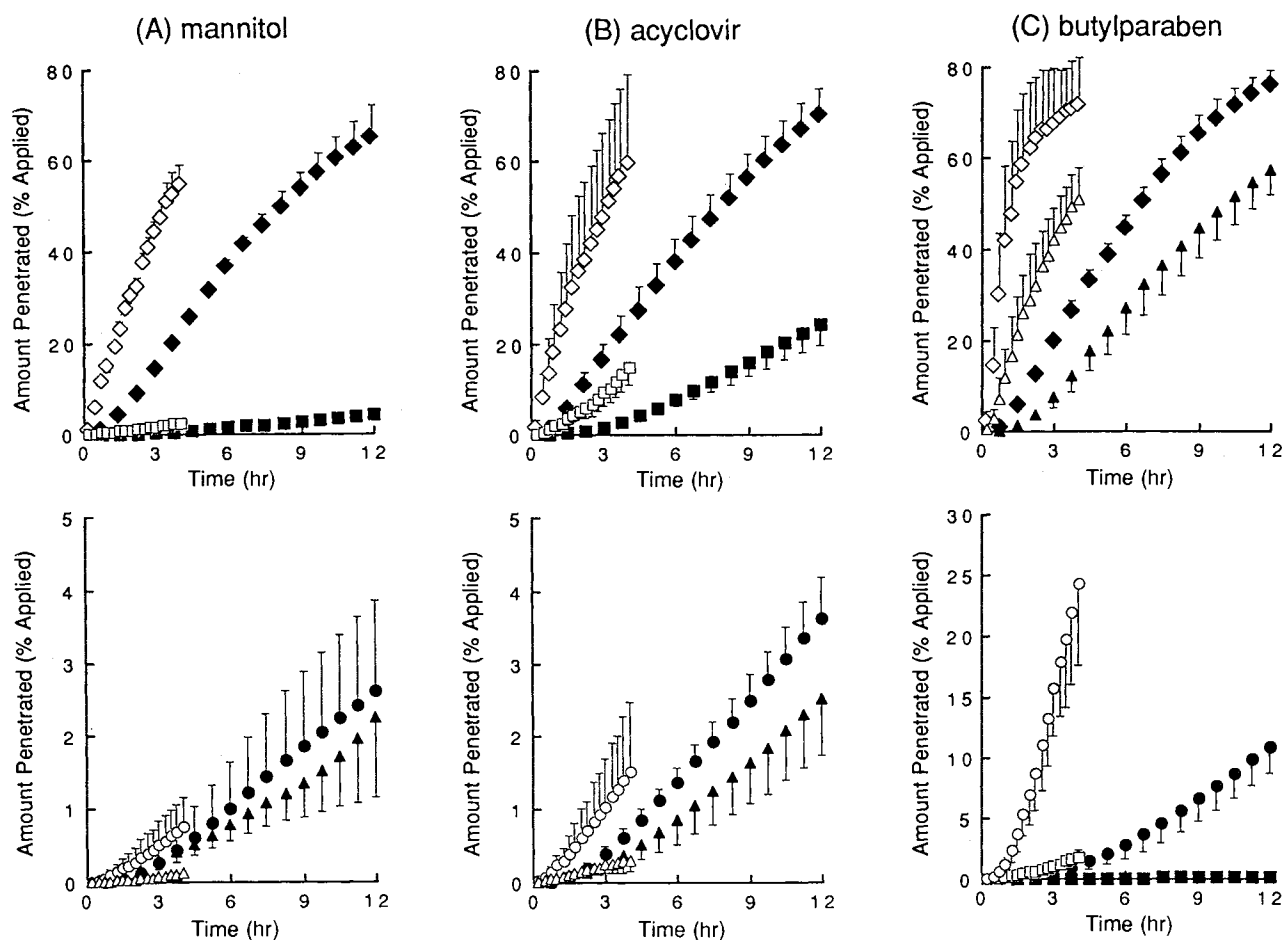


Fig. 2. *In vivo* (open symbols) and *in vitro* (filled symbols) percutaneous penetration of (A) mannitol, (B) acyclovir, and (C) butylparaben through intact guinea pig skin pretreated with an ethanolic solution of 0 μmol (Δ , \blacktriangle), 6.4 μmol (\circ , \bullet), and 51.0 μmol (\square , \blacksquare) of GACH or through tape-stripped skin (\diamond , \blacklozenge). *In vivo* absorption profiles were obtained from urinary excretion data using a deconvolution method. Each point represents the mean value of at least three experiments.

With respect to penetration parameters for the nonpolar route, GACH increased mainly the partition parameters of acyclovir in both experimental systems.

DISCUSSION

In vitro and *in vivo* absorption of three drugs with different lipophilicities through the skin with or without GACH pretreatment was studied based on a two-layer skin model with polar and nonpolar routes in the stratum corneum (20). Concerning drug penetration through a viable layer (tape-stripped skin), diffusion parameters of all drugs were larger and partition parameters were smaller in the *in vivo* system. As expressed in Eqs. (13) and (14), the diffusion parameter is inversely proportional to the second power of diffusion length and the partition parameter is directly proportional to diffusion length. Therefore, assuming that there is no difference in original diffusion and partition coefficients *in vitro* and *in vivo*, this indicates that the diffusion length of a viable layer was shorter *in vivo* than *in vitro*. This result is consistent with the location of the blood capillary at the top of the dermis layer in intact skin.

In most cases, the thickness of a viable layer has little effect on the total skin permeability of drugs, since the rate-limiting step of their passage is at the stratum corneum. For lipophilic drugs, however, it would show a larger effect as observed in an *in vitro* study using split-thickness skin (27). The faster skin penetration of butylparaben in the *in vivo* experiment (Fig. 2) is thus accounted for by the shorter diffusion length in the viable epidermis plus dermis layer. For hydrophilic drugs, the shorter diffusion length was reflected in the shorter lag time of the appearance curve.

The difference in diffusion length in the secondary layer may also affect the apparent enhancer activity. The effect of enhancers on the total drug penetration increases when the barrier function of the diffusion layer that the enhancers affect is strong compared with that of the other barriers.

The polar route in the stratum corneum can be considered to be filled with water (25,26) and the partition coefficient between the polar route and the aqueous vehicle is unity. Therefore, the larger partition parameter for the polar route in the *in vitro* system without GACH pretreatment (Table III) suggests volume enlargement of the polar route. Hydration of the stratum corneum is an important factor in

Table I. Amounts of Drugs Recovered at the End of 12-hr *in Vitro* Diffusion Experiments

Drug	GACH dose (μmol)	Recovery (% applied) ^a			
		Donor	Skin	Receptor	Total
Mannitol	0	92.42 \pm 1.35	0.46 \pm 0.01	2.26 \pm 1.12	95.13 \pm 0.24
	6.4	92.33 \pm 2.51	2.02 \pm 0.97	2.60 \pm 1.26	96.95 \pm 2.63
	51.0	77.55 \pm 4.28	10.67 \pm 1.26	4.28 \pm 0.33	92.50 \pm 2.69
	Stripping	21.50 \pm 3.18	0.68 \pm 0.35	65.25 \pm 6.76	87.43 \pm 9.59
Acyclovir	0	93.70 \pm 2.89	0.95 \pm 0.12	2.51 \pm 0.79	97.15 \pm 2.50
	6.4	92.71 \pm 1.27	1.27 \pm 0.43	3.63 \pm 0.58	97.60 \pm 2.45
	51.0	65.92 \pm 6.60	3.87 \pm 1.22	24.33 \pm 4.65	94.12 \pm 1.34
	Stripping	22.29 \pm 4.35	1.08 \pm 0.52	70.30 \pm 5.77	93.67 \pm 1.10
Butylparaben	0	13.35 \pm 2.79	14.36 \pm 4.38	57.43 \pm 5.55	85.14 \pm 2.52
	6.4	20.15 \pm 4.84	73.81 \pm 11.05	20.15 \pm 4.84	104.78 \pm 7.44
	51.0	9.17 \pm 0.72	71.13 \pm 2.07	0.31 \pm 0.02	80.61 \pm 1.34
	Stripping	10.84 \pm 3.06	1.30 \pm 0.12	76.04 \pm 3.08	88.18 \pm 0.74

^a Data are expressed as the mean \pm SD of at least three experiments.

skin penetration (28), and this effect is more obvious in the *in vitro* study, where the skin is immersed in saline. Lambert *et al.* suggested that long-term hydration led to the development of new polar channels in the stratum corneum and caused an increase in permeability to polar solutes (29).

The partition parameter for the polar route also increased *in vivo* with an increase in the preloading dose of GACH. This suggested that GACH enhances hydration of the stratum corneum. However, since GACH is a lipophilic compound, it is unlikely that GACH directly affects the polar route. It was reported that fatty acids increase transepidermal water loss (TEWL) (30). GACH also might increase the water permeability of the stratum corneum by perturbing its structure and increasing its hydration.

In vivo partition parameters for the polar route approached the corresponding *in vitro* value as the GACH dose increased, suggesting that the water-holding capacity of the stratum corneum is limited. *In vitro* long-term hydration experiments also revealed that the permeability of polar solutes increases with time to a plateau level (30). Since the skin was well hydrated without GACH pretreatment, the effect of

GACH on the polar route was smaller in the *in vitro* system, as observed here for the lower *in vitro* enhancement by GACH of hydrophilic drugs such as acyclovir.

With regard to the nonpolar route in the stratum corneum, there were only small differences in both diffusion and partition parameters for acyclovir between the *in vivo* and the *in vitro* systems without GACH pretreatment. Furthermore, pretreatment with GACH showed similar effects on both parameters *in vitro* and *in vivo* (Table III), i.e., GACH pretreatment increased the partition parameters, depending on its dose, but did not affect the diffusion parameters.

The effect of GACH on drug permeation through the guinea pig skin was reported previously (20). GACH increased mainly the partition parameter of drugs for the nonpolar route, while it barely altered the diffusion parameter (20). The present *in vitro* results in rats agree with these observations, suggesting that the action mechanism of GACH is the same between guinea pigs and rats, both *in vitro* and *in vivo*. The decreased absorption of butylparaben shown *in vitro* and *in vivo* (Fig. 2) also supports these conclusions.

Table II. Amounts of Drugs Recovered at the End of 4-hr *in Vivo* Absorption Experiments

Drug	GACH dose (μmol)	Recovery (% applied) ^a				
		Donor	Skin	Urine	Absorbed ^b	Total ^c
Mannitol	0	86.32 \pm 8.79	0.35 \pm 0.12	0.08 \pm 0.02	0.11 \pm 0.03	86.79 \pm 8.72
	6.4	101.34 \pm 5.08	0.22 \pm 0.07	0.55 \pm 0.31	0.74 \pm 0.41	102.30 \pm 5.40
	51.0	82.76 \pm 15.05	0.52 \pm 0.12	1.74 \pm 0.45	2.48 \pm 0.56	85.76 \pm 15.55
	Stripping	39.29 \pm 2.11	1.09 \pm 0.60	42.06 \pm 3.36	54.67 \pm 4.18	95.05 \pm 1.52
Acyclovir	0	99.08 \pm 1.14	0.32 \pm 0.13	0.24 \pm 0.13	0.30 \pm 0.16	99.70 \pm 1.27
	6.4	97.46 \pm 4.78	0.69 \pm 0.33	1.13 \pm 0.71	1.51 \pm 0.96	101.72 \pm 3.56
	51.0	81.77 \pm 6.89	1.61 \pm 0.01	10.64 \pm 3.04	14.81 \pm 3.88	98.19 \pm 3.02
	Stripping	39.73 \pm 16.24	1.49 \pm 0.48	47.13 \pm 16.35	59.84 \pm 19.29	101.06 \pm 5.05
Butylparaben	0	13.06 \pm 0.70	9.84 \pm 7.28	46.76 \pm 7.26	50.87 \pm 7.06	73.77 \pm 7.74
	6.4	25.47 \pm 2.21	28.96 \pm 7.62	20.37 \pm 5.65	24.23 \pm 6.65	78.67 \pm 1.58
	51.0	16.32 \pm 3.99	51.84 \pm 1.79	1.47 \pm 0.43	1.78 \pm 0.51	69.94 \pm 5.25
	Stripping	6.30 \pm 5.70	1.03 \pm 0.89	70.71 \pm 10.85	71.77 \pm 9.96	79.11 \pm 3.48

^a Data are expressed as the mean \pm SD of at least three experiments.

^b Values were calculated using a deconvolution method (23).

^c Values are the sum of the amounts of drug in the donor, in the skin, and absorbed.

Table III. Estimated Penetration Parameters for Drug Penetration Through Skin Pretreated with Various Doses of GACH Under *in Vitro* and *in Vivo* Conditions

Drug	GACH dose (μmol)	<i>In vitro</i>				<i>In vivo</i>			
		D_p' (hr ⁻¹) ^a	K_p' (×10 ⁵ cm ³) ^b	D_{np}' (hr ⁻¹) ^c	K_{np}' (cm ³) ^c	D_p' (hr ⁻¹) ^a	K_p' (×10 ⁵ cm ³) ^b	D_{np}' (hr ⁻¹) ^c	K_{np}' (cm ³) ^c
Mannitol	0	61.6	6.13	—	—	58.7	0.612	—	—
	6.4	64.6	7.38	—	—	60.2	3.91	—	—
	51.0	64.8	12.2	—	—	60.2	14.5	—	—
	Stripping	$D_d' = 0.0818 \text{ hr}^{-1d}$		$K_d' = 3.67 \text{ cm}^{3d}$		$D_d' = 0.677 \text{ hr}^{-1d}$		$K_d' = 0.368 \text{ cm}^{3d}$	
Acyclovir	0	57.4	6.13	6.57	0.000129	54.7	0.612	6.79	0.000126
	6.4	60.2	7.38	4.71	0.000458	56.1	3.91	5.03	0.000649
	51.0	60.4	12.2	5.14	0.00953	56.1	14.5	4.53	0.0132
	Stripping	$D_d' = 0.0804 \text{ hr}^{-1d}$		$K_d' = 3.76 \text{ cm}^{3d}$		$D_d' = 2.84 \text{ hr}^{-1d}$		$K_d' = 0.0838 \text{ cm}^{3d}$	

^a Diffusion parameters for the polar route in the stratum corneum (D_p'). These values for each drug were calculated by correcting the corresponding values for mannitol based on molecular weight and were also used for calculation of D_{np}' and K_{np}' values of drugs at each GACH dose.

^b Partition parameters for the polar route in the stratum corneum (K_p'). These values for each drug were considered to be the same as the corresponding values for mannitol and were also used for calculation of D_{np}' and K_{np}' values of drugs at each GACH dose.

^c Parameters for the nonpolar route in the stratum corneum (D_{np}' , K_{np}').

^d Parameters for the second viable layer (D_d' , K_d'). These values were considered to be common to each drug with a different GACH dose.

CONCLUSION

The difference between *in vitro* and *in vivo* drug penetration occurs due to the difference in the diffusion length of the epidermis plus dermis layer. Further, the action of GACH on the skin can be attributed to an increase in drug partitioning into the nonpolar route *in vitro* and *in vivo*, and the apparent difference in drug absorption and the enhancer's effect can be attributed largely to different hydration in the stratum corneum *in vitro* and *in vivo*.

Based on the diffusion model and the estimated parameters for each penetration process, it might be possible to predict *in vivo* absorption behavior from *in vitro* data. Since various factors such as metabolism and tissue adsorption could cause *in vitro/in vivo* differences, further investigation will be necessary.

APPENDIX

Based on the model shown in Fig. 1, the mass-balance equation for each domains is expressed as follows;

$$\partial C_p / \partial t = D_p (\partial^2 C_p / \partial x^2) \quad (\text{A1})$$

$$\partial C_{np} / \partial t = D_{np} (\partial^2 C_{np} / \partial x^2) \quad (\text{A2})$$

$$\partial C_d / \partial t = D_d (\partial^2 C_d / \partial x^2) \quad (\text{A3})$$

$$V_b * dC_b / dt = CL / K_d * C_d - (F + CL / K_b) * C_b \quad (\text{A4})$$

where CL and F are clearances for movement through the blood wall and by the blood flow, respectively, and subscript b expresses the blood compartment.

Assuming that the donor and blood compartments are under a well-stirred finite-dose condition, the boundary conditions are given as follows:

$$K_p C_v = C_p \quad (x = -L_s) \quad (\text{A5})$$

$$K_{np} C_v = C_{np} \quad (x = -L_s) \quad (\text{A6})$$

$$V_v (dC_v / dt) = D_p A f (\partial C_p / \partial x) + D_{np} A (1 - f) (\partial C_{np} / \partial x) \quad (x = -L_s) \quad (\text{A7})$$

$$K_d C_p / K_p = C_d \quad (x = 0) \quad (\text{A8})$$

$$K_d C_{np} / K_{np} = C_d \quad (x = 0) \quad (\text{A9})$$

$$D_p A f (\partial C_p / \partial x) + D_{np} A (1 - f) (\partial C_{np} / \partial x) = D_d A (\partial C_d / \partial x) \quad (x = 0) \quad (\text{A10})$$

$$-D_d A (\partial C_d / \partial x) = CL / K_d * C_d - CL / K_b * C_b \quad (x = L_d) \quad (\text{A11})$$

The initial conditions are as follows:

$$C_v = C_0 \quad \text{or} \quad C_v V_v = X_0 \quad (\text{A12})$$

$$C_p = C_{np} = C_d = C_b = 0 \quad (\text{A13})$$

where C_0 and X_0 are the initial concentration and applied amount of drug, respectively.

By taking Laplace transforms, \tilde{Q} , \tilde{X} , \tilde{M}_p , \tilde{M}_{np} , \tilde{M}_d , and \tilde{M}_b are obtained from

$$\begin{aligned} \tilde{Q} &= -D_d A / s * (\partial \tilde{C}_d / \partial x)_{x=L_d} \\ &= W Z_d F X_0 (Z_{np} \sinh d_p + Z_{np} \sinh d_{np}) / s / \\ &\quad (V_b s + F) / k(s) \end{aligned} \quad (\text{A14})$$

$$\begin{aligned} \tilde{X} &= \tilde{C}_v * V_v \\ &= V_v X_0 \{ (Z_{np} \sinh d_p \cosh d_{np} + Z_p \cosh d_p \sinh d_{np}) \\ &\quad (W \sinh d_d + Z_d \cosh d_d) + Z_d \sinh d_p \sinh d_{np} \\ &\quad (W \cosh d_d + Z_d \sinh d_d) \} / s / k(s) \end{aligned} \quad (\text{A15})$$

$$\begin{aligned} \tilde{M}_p &= \int_{-L_s}^0 \tilde{C}_p A f \partial x \\ &= Z_p X_0 \{ \{ Z_p \sinh d_p \sinh d_{np} + Z_{np} (\cosh d_p - 1) \\ &\quad (\cosh d_{np} + 1) \} (W \sinh d_d + Z_d \cosh d_d) + Z_d \sinh d_{np} \\ &\quad (\cosh d_p - 1) (W \cosh d_d + Z_d \sinh d_d) \} / s / k(s) \end{aligned} \quad (\text{A16})$$

$$\begin{aligned} \tilde{M}_{np} &= \int_{-L_s}^0 \tilde{C}_{np} A (1 - f) \partial x \\ &= Z_{np} X_0 \{ \{ Z_{np} \sinh d_p \sinh d_{np} + Z_p (\cosh d_p + 1) \\ &\quad (\cosh d_{np} - 1) \} (W \sinh d_d + Z_d \cosh d_d) \\ &\quad + Z_d \sinh d_p (\cosh d_{np} - 1) (W \cosh d_d \\ &\quad + Z_d \sinh d_d) \} / s / k(s) \end{aligned} \quad (\text{A17})$$

$$\begin{aligned} \bar{M}_d &= \int_0^{L_d} \bar{C}_d A \, dx \\ &= Z_d X_0 (Z_{np} \sinh d_p + Z_p \sinh d_{np}) \{ Z_d \sinh d_d \\ &\quad + W (\cosh d_d - 1) \} / s / k(s) \end{aligned} \quad (A18)$$

$$\begin{aligned} \bar{M}_b &= \bar{C}_b * V_b \\ &= W Z_d V_{bs} X_0 (Z_{np} \sinh d_p + Z_p \sinh d_{np}) / (V_{bs} + F) / s / k(s) \end{aligned} \quad (A19)$$

where

$$W = K_b CL (V_{bs} + F) / s / (K_b V_{bs} + CL + K_b F) \quad (A20)$$

$$\begin{aligned} k(s) &= V_v \{ (Z_p \cosh d_p \sinh d_{np} \\ &\quad + Z_{np} \sinh d_p \cosh d_{np}) (W \sinh d_d + Z_d \cosh d_d) \\ &\quad + Z_d \sinh d_p \sinh d_{np} (W \cosh d_d + Z_d \sinh d_d) \\ &\quad + Z_p \{ Z_p \sinh d_p \sinh d_{np} + Z_{np} (\cosh d_p \cosh d_{np} \\ &\quad - 1) \} (W \sinh d_d + Z_d \cosh d_d) \\ &\quad + Z_d \cosh d_p \sinh d_{np} (W \cosh d_d + Z_d \sinh d_d) \\ &\quad + Z_{np} \{ Z_{np} \sinh d_p \sinh d_{np} \\ &\quad + Z_p (\cosh d_p \cosh d_{np} - 1) \} (W \sinh d_d + Z_d \cosh d_d) \\ &\quad + Z_d \sinh d_p \cosh d_{np} (W \cosh d_d + Z_d \sinh d_d) \} \end{aligned} \quad (A21)$$

Equation (1) is derived from Eq. (A14), assuming that clearances at the blood capillary wall and blood flow are infinitely fast.

REFERENCES

- R. J. Sheuplein and I. H. Blank. Permeability of the skin. *Physiol. Rev.* 51:702-747 (1971).
- AH. Ghanem, H. Mahmoud, W. I. Higuchi, U. D. Rohr, S. Borsadia, P. Liu, J. L. Fox, and W. R. Good. The effects of ethanol on the transport of β -estradiol and other permeants in hairless mouse skin. II. A new quantitative approach. *J. Control. Release* 6:75-83 (1987).
- K. Tojo, C. C. Chiang, and Y. W. Chien. Drug permeation across the skin: Effect of penetrant hydrophilicity. *J. Pharm. Sci.* 76:123-126 (1987).
- H. Okamoto, F. Yamashita, K. Saito, and M. Hashida. Analysis of drug penetration through the skin by the two-layer skin model. *Pharm. Res.* 6:931-937 (1989).
- C. D. Yu, J. L. Fox, N. F. H. Ho, and W. I. Higuchi. Physical model evaluation of topical prodrug delivery—Simultaneous transport and bioconversion of vidarabine-5'-valerate II. Parameter determination. *J. Pharm. Sci.* 68:1347-1357 (1979).
- K. H. Valia, K. Tojo, and Y. W. Chien. Long-term permeation kinetics of estradiol: (III) kinetic analyses of the simultaneous skin permeation and bioconversion of estradiol esters. *Drug Dev. Ind. Pharm.* 11:1133-1173 (1985).
- R. H. Guy, J. Hadgraft, and H. I. Maibach. A pharmacokinetic model for percutaneous absorption. *Int. J. Pharm.* 11:119-129 (1982).
- S. K. Chandrasekaran, W. Bayne, and J. E. Shaw. Pharmacokinetics of drug permeation through human skin. *J. Pharm. Sci.* 67:1370-1374 (1978).
- K. Tojo. Concentration profile in plasma after transdermal drug delivery. *Int. J. Pharm.* 43:201-205 (1988).
- K. Sato, T. Oda, K. Sugibayashi, and Y. Morimoto. Estimation of blood concentration of drugs after topical application from in vitro skin permeation data. II. Approach by using diffusion model and compartment model. *Chem. Pharm. Bull.* 36:2624-2632 (1988).
- K. Sato, T. Oda, K. Sugibayashi, and Y. Morimoto. Estimation of blood concentration of drugs after topical application from in vitro skin permeation data. I. Prediction by convolution and confirmation by deconvolution. *Chem. Pharm. Bull.* 36:2232-2238 (1988).
- T. J. Franz. Percutaneous absorption. On the relevance of in vitro data. *J. Invest. Dermatol.* 64:190-195 (1975).
- R. L. Bronaugh, R. F. Stewart, E. R. Congdon, and A. L. Giles, Jr. Methods for in vitro percutaneous absorption studies I. Comparison with in vitro results. *Toxicol. Appl. Pharmacol.* 62:474-480 (1982).
- R. L. Bronaugh and H. I. Maibach. Percutaneous absorption of nitroaromatic compounds: In vivo and in vitro studies in the human and monkey. *J. Invest. Dermatol.* 84:180-183 (1985).
- R. L. Bronaugh and T. J. Franz. Vehicle effects on percutaneous absorption: In vivo and in vitro comparisons with human skin. *Br. J. Dermatol.* 115:1-11 (1986).
- H. Okamoto, M. Ohyabu, M. Hashida, and H. Sezaki. Enhanced penetration of mitomycin C through hairless mouse and rat skin by enhancers with terpene moieties. *J. Pharm. Pharmacol.* 39:531-534 (1986).
- H. Okamoto, M. Hashida, and H. Sezaki. Structure-activity relationship of 1-alkyl- or 1-alkenylazacycloalkanone derivatives as percutaneous penetration enhancers. *J. Pharm. Sci.* 77:418-424 (1988).
- H. Okamoto, K. Muta, M. Hashida, and H. Sezaki. Percutaneous penetration of acyclovir through excised hairless mouse and rat skin: Effect of vehicle and percutaneous penetration enhancer. *Pharm. Res.* 7:64-68 (1990).
- H. Okamoto, M. Hashida, and H. Sezaki. Effect of 1-alkyl- or 1-alkenylazacycloalkanone derivatives on the penetration of drugs with different lipophilicities in guinea pig skin. *J. Pharm. Sci.* 80:39-45 (1991).
- F. Yamashita, T. Yoshioka, Y. Koyama, H. Okamoto, H. Sezaki, and M. Hashida. Analysis of skin penetration enhancement based on a two-layer skin diffusion model with polar and nonpolar routes in the stratum corneum: Dose-dependent effect of 1-geranylazacycloheptan-2-one on drugs with different lipophilicities. *Biol. Pharm. Bull.* 16:690-697 (1993).
- F. Yamashita, Y. Koyama, H. Sezaki, and M. Hashida. Estimation of a concentration profile of acyclovir in the skin after topical administration. *Int. J. Pharm.* 89:199-206 (1993).
- H. Kiwada, K. Morita, M. Hayashi, S. Awazu, and M. Hanano. A new numerical calculation method for deconvolution in linear compartment analysis of pharmacokinetics. *Chem. Pharm. Bull.* 25:1312-1318 (1977).
- R. T. Tregear. *Physical Functions of Skin*, Academic Press, New York, 1966, pp. 1-52.
- Y. Yano, K. Yamaoka, and H. Tanaka. A nonlinear least square program, MULTI(FILT), based on fast inverse Laplace transform for microcomputers. *Chem. Pharm. Bull.* 37:1035-1038 (1989).
- C. Ackermann and G. L. Flynn. Ether-water partitioning and permeability through nude mouse skin in vitro. I. Urea, thio-urea, glycerol and glucose. *Int. J. Pharm.* 36:61-66 (1987).
- C. Ackermann, G. L. Flynn, and W. M. Smith. Ether-water partitioning and permeability through nude mouse skin in vitro. II. Hydrocortisone 21-n-alkyl esters, alkanols and hydrophilic compounds. *Int. J. Pharm.* 36:67-71 (1987).
- R. L. Bronaugh and R. F. Stewart. Methods for in vitro percutaneous absorption studies. VI. Preparation of the barrier layer. *J. Pharm. Sci.* 75:487-491 (1986).
- B. Idson. Percutaneous absorption. *J. Pharm. Sci.* 64:901-924 (1975).
- W. J. Lambert, W. I. Higuchi, K. Knutson, and S. L. Krill. Effects of long-term hydration leading to the development of polar channels in hairless mouse stratum corneum. *J. Pharm. Sci.* 78:925-928 (1989).
- P. G. Green, R. H. Guy, and J. Hadgraft. In vitro and in vivo enhancement of skin permeation with oleic and lauric acids. *Int. J. Pharm.* 48:103-111 (1988).